Abdominal Radiology (2025) 50:2388–2400
https://doi.org/10.1007/s00261-024-04710-0

RESEARCH

MRI-based radiomic nomogram for predicting disease-free survival in patients with locally advanced rectal cancer

Jun Liu[1] · Ke Liu[2] · Fang Cao[3] · Pingsheng Hu[1] · Feng Bi[1] · Siye Liu[1] · Lian Jian[1] · Jumei Zhou[2] · Shaolin Nie[4] · Qiang Lu[1] · Xiaoping Yu[1] · Lu Wen[1]

Received: 27 August 2024 / Revised: 15 November 2024 / Accepted: 16 November 2024 / Published online: 4 December 2024

Abstract

Purpose Individual prognosis assessment is of paramount importance for treatment decision-making and active surveillance in cancer patients. We aimed to propose a radiomic model based on pre- and post-therapy MRI features for predicting disease-free survival (DFS) in locally advanced rectal cancer (LARC) following neoadjuvant chemoradiotherapy (nCRT) and subsequent surgical resection.

Methods This retrospective study included a total of 126 LARC patients, which were randomly assigned to a training set (n = 84) and a validation set (n = 42). All patients underwent pre- and post-nCRT MRI scans. Radiomic features were extracted from higher resolution T2-weighted images. Pearson correlation analysis and ANOVA or Relief were utilized for identifying radiomic features associated with DFS. Pre-treatment, post-treatment, and delta radscores were constructed by machine learning algorithms. An individualized nomogram was developed based on significant radscores and clinical variables using multivariate Cox regression analysis. Predictive performance was evaluated by the C-index, calibration curve, and decision curve analysis.

Results The results demonstrated that in the validation set, the clinical model including pre-surgery carcinoembryonic antigen (CEA), chemotherapy after radiotherapy, and pathological stage yielded a C-index of 0.755 (95% confidence interval [CI]: 0.739–0.771). While the optimal pre-, post-, and delta-radscores achieved C-indices of 0.724 (95%CI: 0.701–0.747), 0.701 (95%CI: 0.671–0.731), and 0.625 (95%CI: 0.589–0.661), respectively. The nomogram integrating pre-surgery CEA, pathological stage, alongside pre- and post-nCRT radscore, obtained the highest C-index of 0.833 (95%CI: 0.815–0.851). The calibration curve and decision curves exhibited good calibration and clinical usefulness of the nomogram. Furthermore, the nomogram categorized patients into high- and low-risk groups exhibiting distinct DFS (both $P < 0.0001$).

Conclusions The nomogram incorporating pre- and post-therapy radscores and clinical factors could predict DFS in patients with LARC, which helps clinicians in optimizing decision-making and surveillance in real-world settings.

Keywords Locally advanced rectal cancer · Disease-free survival · MRI · Radiomic

Introduction

Colorectal cancer is a significant global health challenge, ranking as the third most common cancer and the second leading cause of cancer-related deaths worldwide [1]. This underscores the urgent need for comprehensive understanding and effective interventions for this disease. Notably, rectal cancer is responsible for around 30% of all colorectal cancer cases [2]. The established protocol for treating locally advanced rectal cancer (LARC) is neoadjuvant chemoradiotherapy (nCRT) with subsequent total mesorectal excision (TME) [3]. This treatment approach has significantly reduced the incidence of local recurrence to less than 10% [4, 5]. Yet, despite these advancements, challenges persist, particularly in terms of survival rates and the occurrence of distant metastasis, which remain significant concerns for patients diagnosed with LARC [6, 7]. Patients with high-risk factors may receive recommendations for neoadjuvant chemotherapy before surgery and adjuvant chemotherapy after surgery. This approach aims to mitigate the risk of distant metastasis and improve disease-free survival (DFS), ultimately contributing to an overall survival benefit [8, 9]. Nonetheless, it is crucial to recognize that not all patients will benefit from additional chemotherapy. Thus, accurate

Extended author information available on the last page of the article

prognosis identification is crucial to make personalized treatment strategies for LARC patients.

Presently, the conventional TNM staging system serves as the conventional measure for risk stratification and treatment allocation in cancer. However, its precision is limited due to its reliance solely on anatomical information [6, 10]. Recognizing this limitation, numerous studies have delved into the exploration of additional prognostic indicators, encompassing serological, clinical, and pathological features. This expanded approach aims to provide a more comprehensive understanding of survival outcomes for patients diagnosed with rectal cancer [11–13]. However, even with strict adherence to these guidelines, the DFS rate continues to exhibit variability, ranging from 64.5% to 76% [14–16]. This discrepancy may be attributed to the fact that these risk factors fail to consider the inherent biological heterogeneity of LARC. The integration of data from diverse perspectives suggests that a prediction model has the potential to achieve improved performance in risk stratification, considering the multifaceted nature of the disease.

Radiomics, through the high-throughput extraction of deep-seated feature representations from medical images, can reveal hidden features that are not visible to the naked eye [17, 18]. The quantitative radiomic features are able to further reflect the biological characteristics of tumors and be utilized in the evaluation of therapeutic effects and prognosis [19]. Previous studies have shown the potential of radiomic analysis based on pre-therapy computed tomography (CT) or conventional magnetic resonance imaging (MRI) in predicting survival in LARC patients [20–24]. Nevertheless, there is a limited body of research investigating the value of post-therapy and delta radiomic features. Therefore, this research dealt with investigating the prognostic value of pre- and post-therapy MRI-based radiomic features in predicting DFS in patients with LARC.

Materials and methods

Patients

The approval for the retrospective study was granted by the institutional review board of our hospital, and waived the requirement for informed consent. All methods were performed in accordance with the relevant guidelines and regulations. A thorough assessment of consecutive patients who had undergone surgical resection at a single tertiary cancer hospital was conducted within the timeframe spanning from July 22, 2014, to June 15, 2018. The criteria for inclusion of patients were listed below: (1) pathology-confirmed newly diagnosed rectal cancer; (2) clinical stage II to III (cT3-4M0 and/or positive nodal status) at pre-nCRT MRI scan; (3) designated for nCRT prior to surgical resection; (4) underwent total mesorectal excision with postoperative pathological assessment after completion of nCRT; and (5) pre- and post-nCRT MRI images were available. The criteria for exclusion were listed below: (1) prior anti-cancer therapy; (2) poor image quality due to stent insertion; and (3) a time duration exceeding 12 weeks between post-nCRT MRI and surgery. Ultimately, 126 patients meeting these criteria were eligible for inclusion and were subjected to subsequent analysis (Fig. 1).

The clinical data encompassed a range of parameters, comprising gender, clinical T (cT) stage, N (cN) stage, TNM (cTNM) stage, age, and pathological type (well- and moderately- differentiated adenocarcinoma, and poorly-undifferentiated adenocarcinoma, signet ring cell carcinoma, and others). Additionally, markers including carcinoembryonic antigen (CEA) and carbohydrate antigen-199 (CA199) assessed pre-nCRT and pre-surgery. Chemotherapy-related variables included whether chemotherapy was administered before radiotherapy (yes or no), chemotherapy cycles, and modalities prior to radiotherapy (none, XELOX, mFOLFOX6). Similarly, chemotherapy after radiotherapy was characterized by its administration (yes or no), number of cycles, and modalities (XELOX, mFOLFOX6, Folfox6). Post-surgery parameters encompassed pathological stage (pT, pN, pTNM stage), and response (pCR or non-pCR), as well as administration of chemotherapy after surgery (yes or no), including its cycle number and modalities (none, XELOX, mFOLFOX6, Folfox6). This comprehensive array of clinical variables provides a thorough foundation for subsequent analyses. Wen L, et al. have described detailed information regarding adjuvant chemoradiotherapy strategies and pathological response assessment methods [25]. The clinical endpoint was DFS, which was defined as the duration from surgery until either disease progression or fatality from any cause.

MRI image acquisition

The included patients were assessed through rectal MRI at two specific time points: 1–3 days prior to the commencement of the nCRT (ie, pre-nCRT MRI) and 2–5 days prior to the surgery (ie, post-nCRT MRI). Two GE Healthcare Systems, specifically a 3.0 T Optima® Discovery MR750, and a 1.5 T Optima® MR360, both equipped with a phase-array coil, were utilized to acquire MR images. High-resolution T2-weighted images were acquired by employing a respiratory-triggered fast spin echo sequence, allowing for detailed visualization in sagittal, axial, oblique-coronal, and oblique-axial orientations. The parameters used were as follows: Repetition Time / Echo Time (TR/TE) of 2000–3000/120 ms, a field of view (FOV) measuring 240 mm × 240 mm, an acquisition matrix of 320 × 320, a

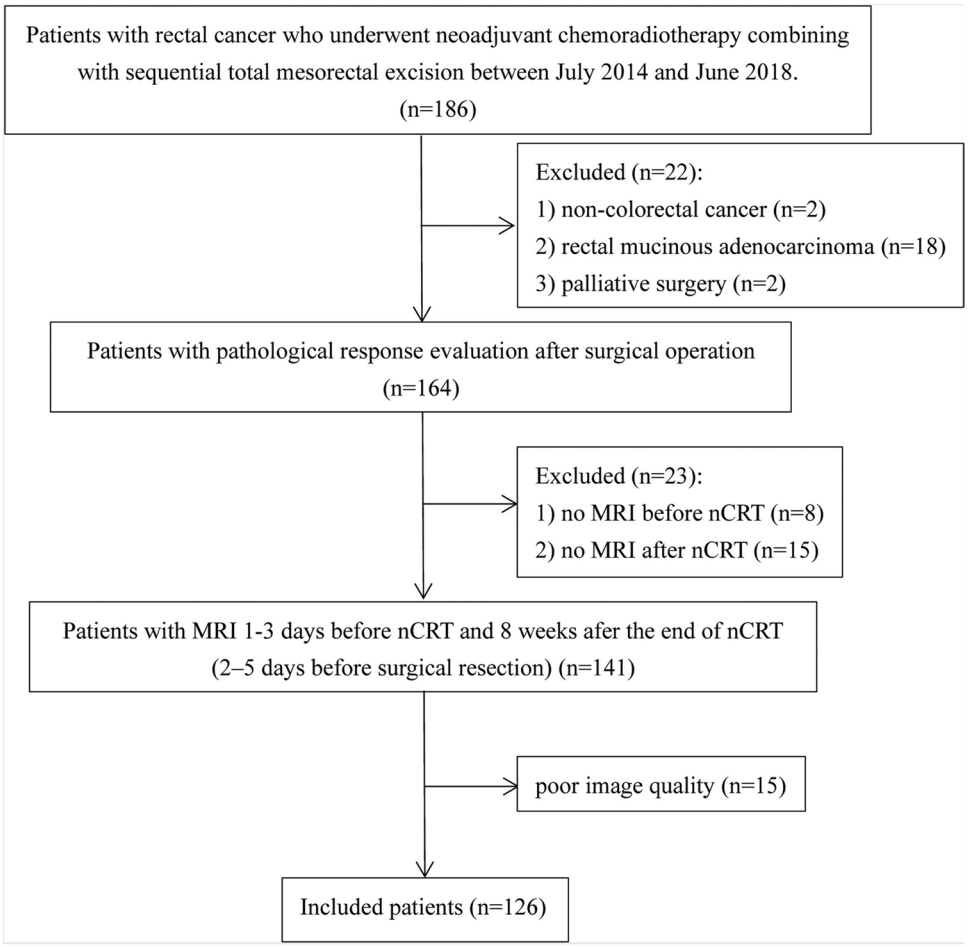

Fig. 1 Flowchart summarizes patient selection and allocation to the training and validation sets

flip angle of 90°, a slice gap of 0.5 mm and section thickness of 3 mm. This imaging protocol not only provided high spatial resolution but also ensured comprehensive coverage of the rectal anatomy, enabling a thorough examination of structural changes with precision and clarity.

MRI image segmentation

The T2-weighted DICOM images underwent conversion to Bitmap format and were then imported into a software utilized for radiomic analyses, MaZda (v 4.6.2, https://qmazda.p.lodz.pl/index.php?action=mazda_46). A board-certified radiologist, with a decade of expertise in rectal MRI, was responsible for manually delineating the regions of interest (ROIs) on every slice. During the process, the radiologist carefully chose not to incorporate regions that might introduce ambiguity or uncertainty due to difficulty in accurately identifying the normal rectal wall or exhibiting the presence of mucosal edema when assessing oblique-axial T2-weighted images. The outcome of this meticulous procedure resulted in the generation of a volume of interest for each case. MRI data (pre- and post-nCRT) were employed for the purpose of image segmentation and extraction of pertinent features, ensuring a comprehensive and thorough analysis. The segmentation outcomes underwent thorough scrutiny by a senior radiologist with extensive expertise in the field of rectal MRI (15 years). Any discrepancies were meticulously addressed and resolved through a collaborative consensus-based discussion. The criteria for reaching consensus involved revisiting the imaging data, comparing the segmentation results to established the final version. This rigorous approach ensured a thorough examination of the segmentation outcomes and the resolution of any differences in interpretation or analysis.

Extraction and selection of features, and radiomic signature establishment

The VOIs were identified in oblique-axial T2WI images obtained from the MRI data (pre- and post-nCRT). These were then comprehensively assessed resulting in 250 radiomic features being extracted. These can be categorized into the given five types: (1) **First-order histogram**: encompassing variance, mean, kurtosis, skewness, and percentiles (1-%, 10-%, 50-%, 90-%, and 99-%); (2) **Absolute gradient**: encompassing variance, mean, kurtosis,

skewness, and percentage of pixels with a nonzero gradient; (3) **Run-length matrix (RLM)**: encompassing grey level nonuniformity (GLevNonU), run length nonuniformity (RLNonUni), short-run emphasis (ShrtREmph), long run emphasis (LngREmph), and fraction of image in runs (Fraction); (4) **Gray-level co-occurrence matrix (GLCM):** encompassing angular second moment (AngScMom), contrast, correlation, sum of squares (SumOfSqs), inverse difference moment (InvDfMom), sum variance (SumVarnc), sum average (SumAverg), entropy, sum entropy (SumEntrp), difference entropy (DifEntrp) and difference variance (DifVarnc); and (5) **AR model**: encompassing θ1, θ2, θ3, θ4, and σ. Furthermore, the Z-score was utilized for the standardization of the radiomic features. Additionally, a delta-radiomic feature was defined as the change in a specific radiomic feature from pre- to post-nCRT MRI.

Pearson correlation was performed for the random exclusion of a feature within feature pairs displaying strong redundancy, using 0.99 as the threshold. This was done to diminish feature dimensionality. Subsequently, continual dimensionality reduction was applied to the retained features by utilizing either ANOVA or the relief feature selection method, aiming to determine candidate predictors of DFS. Following this, a comparative assessment of five machine-learning classifiers (ie, Gaussian Processes (GP), Adaboost, support vector machines (SVM), Naive Bayes (NB), and logistic regression (LR)) was executed in order to establish pre-, post-, and delta-radiomic models with excellent performance. The area under the curve (AUC) was employed as a key metric to evaluate the performance of the five classifiers in relation to the selected features. This process involved optimizing hyperparameters and selecting the best classifier through a stratified fivefold cross-validation method conducted within the training set. To ensure the reliability and generalizability of our models, we conducted validation with an independent set to obtain the final models.

Development and validation of radiomic nomogram

A radiomic nomogram was developed through a comprehensive process that involved screening pertinent clinical parameters and three radscores through multivariable Cox regression analysis, using the Akaike Information Criterion (AIC) as the standard for variable selection. To ensure the reliability of predictions, calibration curves were employed to evaluate the alignment between predicted and observed outcomes. Stratification of patients into high- or low-risk groups was achieved based on the optimal cutoff value computed by the X-tile 3.6.1 (https://medicine.yale.edu/lab/rimm/research/software/), enhancing the accuracy of risk assessment in this context. The cutoff value was defined in the training set with subsequent application to the validation set. Patients with a score surpassing the cut-point were categorized into the high-risk group, whereas those with a score below the cut-point were categorized into the low-risk group. Kaplan-Meier curves were formulated to validate the effectiveness of risk stratification, both in the training and validation sets. The Log-rank test was utilized for comparative assessment of the Kaplan-Meier curves. Decision curve analysis (DCA) was done to gain a comprehensive understanding of the net benefit associated with employing particular strategies in clinical settings.

Statistical analysis

All statistical analyses were done using R software (v3.4.1; http://www.Rproject.org). Diverse statistical techniques were applied to make comparisons between continuous and categorical variables, including the Mann-Whitney U test, t-test, or Chi-square test, as appropriate. The analysis was further reinforced through the utilization of distinct R packages, with "glmnet" employed for the development of classifiers, "rms" employed for conducting multivariable Cox regression analysis and the generation of calibration curves, and "rmda" adopted for the execution of DCA. $P < 0.05$ was deemed as a statistically significant value.

Results

Patient characteristics

Out of 186 patients, 60 were excluded, resulting in a final sample size of 126 patients. The patients were randomly divided into training (n = 84, mean age ± standard deviation, 50.8 years ± 11.0; 61 men) and validation (n = 42, mean age, 51.4 years ± 8.6; 24 men) groups, with a ratio of approximately 2:1. Among the 126 patients, 85 (67.5%) were male, and the median age was recorded to be 51.0 years, with an age range spanning from 21 to 73 years and an interquartile range between 44.3 and 57.0 years. A summary of patient and tumor features is accessible in Table 1**.** Histopathologic examination revealed that 22.2% of the patients (28/126) achieved a pCR, all demonstrating ypT0 (Dworak grade 4). The distribution of Dworak grades among the patients was as follows: 5 (4.0%) with grade 0, 39 (31.0%) with grade 1, 39 (31.0%) with grade 2, and 15 (11.9%) with grade 3. There were no considerable variations in the pertinent features of patients across the training and validation sets (Table 1).

Pre-, post-, and delta-radiomic signatures

The optimal pre-nCRT radiomic signature, employing ANOVA as the feature selection method and GP as the classifier, consisted of ten radiomic features. These

Table 1 Patient characteristics

	Training cohort (n = 84)	Validation cohort (n = 42)	*P*-value
Sex			0.080
Male	61 (72.6)	24 (57.1)	
Female	23 (27.4)	18 (42.9)	
Age (years)*	51.0 ± 11.0	51.4 ± 8.6	0.751
Pre-nCRT CEA (mg/L)†	3.7 (1.4, 7.5)	4.5 (2.6, 8.9)	0.243
Pre-surgery CEA (mg/L) †	1.1 (0.7, 1.9)	1.5 (1.0, 2.7)	0.101
Pre-nCRT CA199 (u/ml) †	9.0 (5.4, 28.3)	9.2 (4.5, 25.7)	0.664
Pre-surgery CA199 (u/ml) †	7.4 (4.0, 12.8)	8.3 (3.4, 16.8)	0.725
Pathological type			0.842
Well-differentiated adenocarcinoma	5 (6.0)	4 (9.5)	
Moderately differentiated adenocarcinoma	55 (65.5)	27 (64.3)	
Poorly-undifferentiated adenocarcinoma	11 (13.1)	4 (9.5)	
Signet ring cell carcinoma	1 (1.2)	0	
Others	12 (14.3)	7 (16.7)	
Chemotherapy before radiotherapy			0.449
Yes	42 (50.0)	24 (57.1)	
No	42 (50.0)	18 (42.9)	
Cycles of chemotherapy before radiotherapy			0.781
0	42 (50.0)	18 (42.9)	
1	33 (39.3)	20 (47.6)	
2	8 (9.5)	4 (9.5)	
3	1 (1.2)	0	
Chemotherapy modalities before radiotherapy			0.198
None	42 (50.0)	18 (42.9)	
XELOX	41 (48.8)	21 (50.0)	
mFOLFOX6	1 (1.2)	3 (7.1)	
Chemotherapy after radiotherapy			0.407
Yes	13 (15.5)	9 (21.4)	
No	71 (84.5)	33 (78.6)	
Cycles of chemotherapy after radiotherapy			0.331
0	71 (84.5)	33 (78.6)	
1	1 (1.2)	3 (7.1)	
2	9 (10.7)	5 (11.9)	
3	3 (3.6)	1 (2.4)	
Chemotherapy modalities after radiotherapy			0.550
None	71 (84.5)	33 (78.6)	
XELOX	10 (11.9)	6 (14.3)	
mFOLFOX6	0	1 (2.4)	
FOLFOX6	3 (3.6)	2 (4.8)	
Pathological response			0.880
pCR	19 (22.6)	9 (21.4)	
Non-pCR	65 (77.4)	33 (78.6)	
Chemotherapy after surgery			1.000
Yes	54 (64.3)	27 (64.3)	
No	30 (35.7)	15 (35.7)	
Cycles of chemotherapy after surgery			0.436
0	30 (35.7)	15 (35.7)	
1	10 (11.9)	3 (7.1)	
2	5 (6.0)	4 (9.5)	
3	5 (6.0)	3 (7.1)	

Table 1 (continued)

	Training cohort (n = 84)	Validation cohort (n = 42)	*P*-value
4	8 (9.5)	1 (2.4)	
5	9 (10.7)	4 (9.5)	
6	9 (10.7)	10 (23.8)	
7	5 (6.0)	2 (4.8)	
8	3 (3.6)	0	
Chemotherapy modalities after surgery			0.887
None	30 (35.7)	15 (35.7)	
XELOX	18 (21.4)	11 (26.2)	
mFOLFOX6	16 (19.0)	6 (14.3)	
Folfox6	20 (23.8)	10 (23.8)	
cT stage			0.617
2	2 (2.4)	0	
3	40 (47.6)	18 (42.9)	
4	42 (50.0)	24 (57.1)	
cN stage			0.168
0	5 (6.0)	0	
1	79 (94.0)	42 (100.0)	
cTNM stage			0.300
2	4 (4.8)	0	
3	80 (95.2)	42 (100.0)	
pT stage			0.988
0	24 (28.6)	11 (26.2)	
1	3 (3.6)	1 (2.4)	
2	22 (26.2)	12 (28.6)	
3	20 (23.8)	11 (26.2)	
4	15 (17.9)	7 (16.7)	
pN stage			0.648
0	55 (65.5)	29 (69.0)	
1	16 (19.0)	9 (21.4)	
2	13 (15.5)	4 (9.5)	
pTNM stage			0.222
0	18 (21.4)	11 (26.2)	
1	14 (16.7)	12 (28.6)	
2	23 (27.4)	6 (14.3)	
3	29 (34.5)	13 (31.0)	

pCR pathological complete response, *CEA* carcinoembryonic antigen, *CA199* carbohydrate antigen-199

Unless otherwise specified, data are numbers of patients, with percentages in parentheses

*Data are means ± standard deviations

†Data are medians, with interquartile ranges in brackets

features encompassed S(0,1)SumOfSqs, Area_S(1,−1), S(1,−1)SumOfSqs, S(0,2)SumOfSqs, Area_S(2,−2), S(2,−2)SumOfSqs, Area_S(3,−3), Area_S(4,−4), S(0,5) SumVarnc, and Area_S(5,−5).

The post-nCRT radiomic signature, identified using Relief as the feature selection method and AdaBoost as the classifier, demonstrated the optimal performance, incorporating three radiomic features, including Skewness, S(1,−1)Correlat, and S(0,3)Correlat.

The optimal delta-radiomic signature, where the change between pre- and post-nCRT radiomic characteristics was analyzed, was developed through the utilization of ANOVA as the feature selection method and NB as the classifier. This signature was composed of 12 radiomic features, encompassing S(0,1)SumOfSqs, S(1,−1)DifEntrp, S(0,2)

SumOfSqs, S(2,−2)DifEntrp, S(3,−3)Contrast, S(3,−3) InvDfMom, S(0,4)SumOfSqs, S(0,4)SumVarnc, S(0,4) SumEntrp, Area_S(4,−4), S(4,−4)Contrast, and S(0,5) SumVarnc.

Within the training set, the pre-, post-, and delta-radiomic signatures demonstrated robust predictive performance, as evidenced by C-indices of 0.835 (95%CI: 0.818–0.852), 0.940 (95%CI: 0.930–0.950), and 0.784 (95%CI: 0.765–0.803), respectively. Conversely, in the validation set, all three radiomic signatures exhibited the capacity to predict DFS in patients with LARC. Their respective C-indices were 0.724 (95%CI: 0.701–0.747), 0.701 (95%CI: 0.671–0.731), and 0.625 (95%CI: 0.589–0.661) (Table 2). Among these signatures, it is noteworthy that the pre-nCRT radiomic signature exhibited the highest discriminatory capacity in the validation set (Table 2).

Predictive performance of the radiomic nomogram

An assessment of clinical variables through univariate Cox analysis revealed that several factors exhibited statistical significance in predicting outcomes. Specifically, pre-nCRT CEA ($P = 0.032$), pre-surgery CEA ($P = 0.003$), the administration of chemotherapy after radiotherapy ($P = 0.047$), pN stage ($P = 0.005$), and pTNM stage ($P = 0.003$) all emerged as statistically significant predictors. As per the results of the multivariate Cox analysis, it was determined that pre-surgery CEA, the inclusion of chemotherapy after radiotherapy, and the pTNM stage retained their statistical significance and were selected for the building of the clinical model. In the training set, the clinical model demonstrated a C-index of 0.802 (95%CI: 0.775–0.829), while the value was 0.755 (95%CI: 0.739–0.771) for the validation set.

Table 2 Performance of clinical model, radiomic scores and nomogram in the prediction of DFS

Models	C-index (95%CI)	*P*-value
Training cohort		
Clinical model	0.802 (0.775–0.829)	<0.001*
Pre-nCRT radscore	0.835 (0.818–0.852)	<0.001*
Post-nCRT radscore	0.940 (0.930–0.950)	0.592
Delta radscore	0.784 (0.765–0.803)	<0.001*
Radiomic nomogram	0.924 (0.910–0.938)	Ref
Validation cohort		
Clinical model	0.755 (0.739–0.771)	<0.001*
Pre-nCRT radscore	0.724 (0.701–0.747)	<0.001*
Post-nCRT radscore	0.701 (0.671–0.731)	<0.001*
Delta radscore	0.625 (0.589–0.661)	<0.001*
Radiomic nomogram	0.833 (0.815–0.851)	Ref

DFS disease-free survival, *nCRT* neoadjuvant chemoradiotherapy

The radiomic nomogram was established by integrating the following variables: pre-surgery CEA ($P = 0.004$), pTNM stage ($P = 0.010$), pre-nCRT radscore ($P = 0.006$), and post-nCRT radscore ($P = 0.007$) (Fig. 2a). The radiomic nomogram demonstrated superior predictive performance, as evidenced by a C-index of 0.833 (95%CI: 0.815–0.851), surpassing both the C-index of the clinical model and those of the three radiomic signatures ($P < 0.001$) (Table 2). Additionally, calibration curves illustrated good alignment between the prediction and actual observations of the nomogram (Fig. 2b and c). The DCA indicated that the clinical utility of the radiomic nomogram exceeded that of the other models (Fig. 2d). Comparatively, in comparison to the clinical and radiomic models, the nomogram exhibited enhanced stratification capabilities for patients with LARC in both the training and validation cohorts. Using a cutoff value of 0.62, it could effectively segregate LARC patients into distinct high- and low-risk subgroups, presenting remarkably different DFS probabilities ($P = 3e\text{-}08$ and $P = 2e\text{-}06$) (Fig. 3). The ROC curves at the 5-year mark further corroborated the exceptional predictive accuracy of the nomogram, as depicted in Fig. 4.

Discussion

The objective of this current research was to establish and verify the predictive significance of MRI-based radiomic in the context of patients with LARC. The findings of this research indicate that incorporating pre-therapy and post-therapy radiomic signatures into the prognostic evaluation model improves risk stratification compared to clinical models alone. The radiomic nomogram emerged as a highly effective and sophisticated tool, effectively categorizing LARC patients into two distinct and clearly delineated risk subgroups. These subgroups, each characterized by their own unique survival profiles, offer profound insights into the dynamic nature of disease progression within this patient population. This research provides a reliable tool for personalized management of patients with LARC in the future.

LARC is characterized by a high degree of clinical heterogeneity, resulting in varying outcomes, even among patients sharing the same disease stage. Given this inherent variability, precise prognostic assessment assumes paramount importance in guiding and tailoring treatment strategies. In pursuit of this objective, prior investigations have delved into the area of texture analysis, assessing data from various imaging modalities, as a means to predict survival outcomes in LARC patients [26, 27]. Omer et al.[26] found that MR-based textural features of rectal cancer can predict outcomes before surgical intervention and have the potential to guide individualized therapy selection. Similarly,

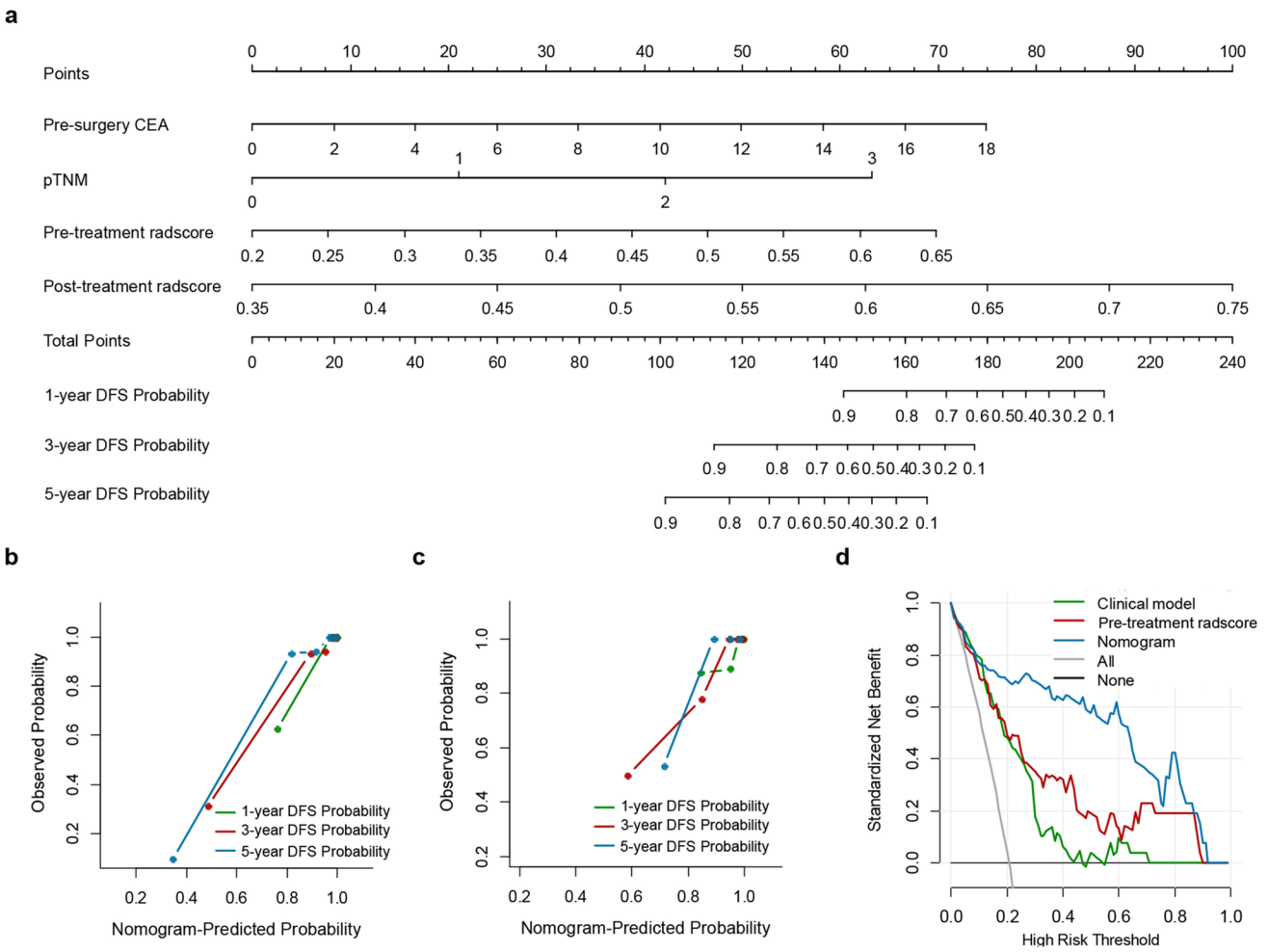

Fig. 2 The nomogram for predicting the probability of 3-year and 5-year DFS. **a** nomogram; **b** calibration curve of training cohort; **c** calibration curve of validation cohort; **d** clinical decision curve

Lovinfosse et al.[27] conducted a study that further underscores the significance of texture analysis. Their research specifically highlighted the application of baseline 18F-FDG PET/CT texture analysis as a powerful tool for identifying and establishing robust, independent predictors of survival among patients with LARC.

Currently, several studies have attempted to build radiomic models to predict survival in patients with LARC [20–24]. These studies extracted texture parameters from different imaging modalities, including CT and MRI. The study developed a radiomic model exclusively based on high-resolution T2WI. This imaging technique offers remarkable advantages by effectively distinguishing between tumor and fibrosis in rectal cancer specimens, playing a pivotal role in the comprehensive evaluation and local staging of rectal cancer [28]. Notably, DCE imaging was not integrated into our study methodology. This omission was due to its absence from routine MRI protocols used for the diagnosis and staging of rectal cancer. While certain functional MRI sequences, like DWI, have shown potential value in predicting survival among patients with LARC, their reliability and stability were compromised by susceptibility artifacts or distortion. These technical issues could significantly impact tumor segmentation and the extraction of pertinent features, undermining the consistency and robustness of the data acquired from these sequences [29, 30]. Thus, this study opted for the utilization of T2WI images as a choice for evaluating clinical outcomes in rectal cancer, primarily due to their immense practical applicability. Tibermacine et al.[22] conducted an investigation where they explored the development of three distinct radiomic models exclusively based on T2WI. Their resulting data indicated that these models exhibited superior performance, characterized by AUC values ranging from 0.77 to 0.89 when predicting DFS. Notably, the performance observed in these T2WI-based models was not significantly different from that achieved by the more complex multi-parameter approach and, interestingly, surpassed the performance of CT imaging. Similarly,

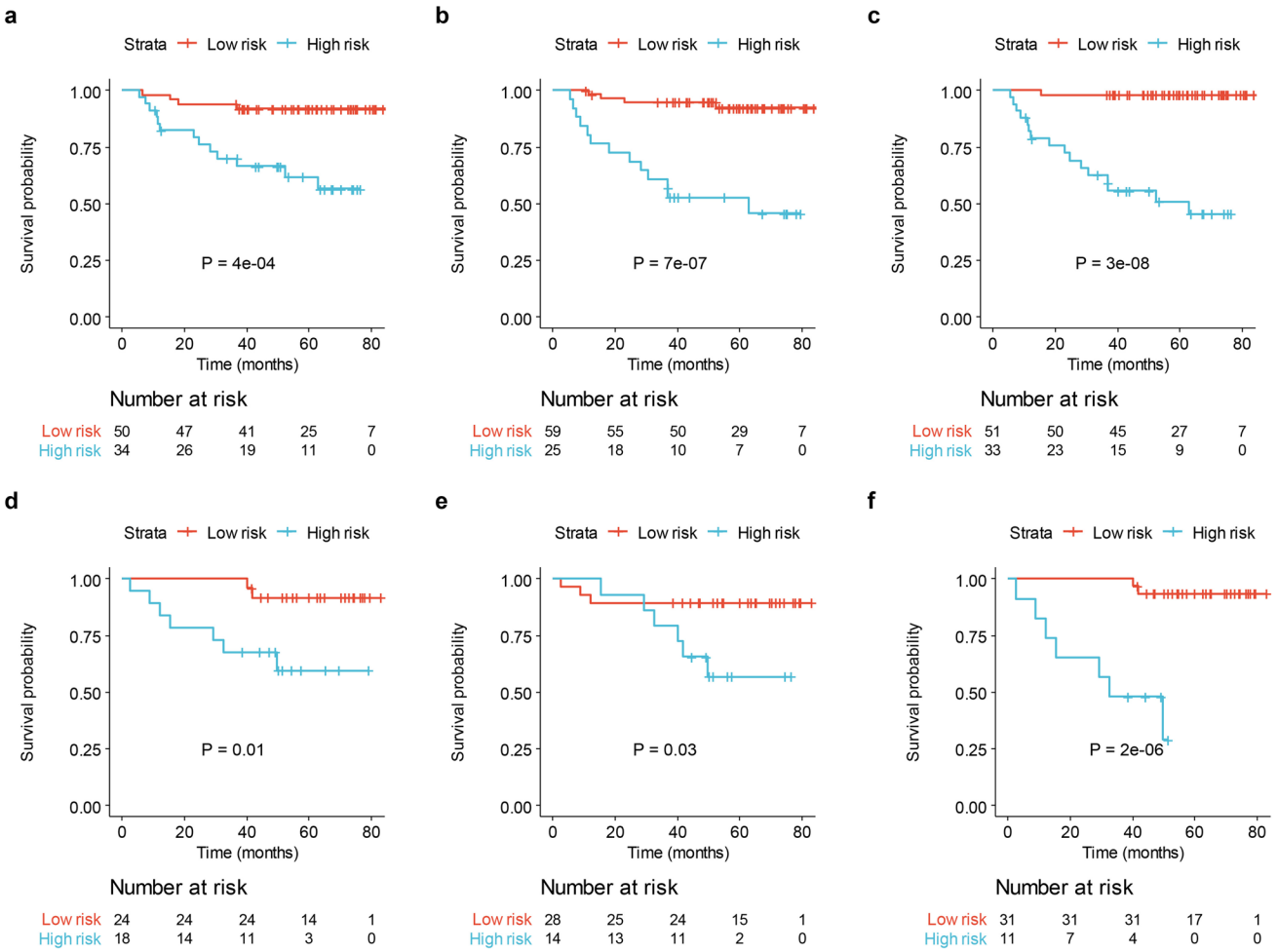

Fig. 3 Kaplan-Meier survival curves of high-risk and low-risk subgroups stratified by the clinical model, the radiomic model, and nomogram in the training set (**a**–**c**) and validation cohort (**d**–**f**)

in this study, the radiomic model based on T2WI showed promising capacity to predict DFS following nCRT.

Furthermore, this research extracted radiomic features from pre- and post-therapy MRI images and established three corresponding signatures to predict DFS in LARC patients. The predictive metrics of the pre-, post-, and delta-radiomic signatures were also compared for predicting DFS. The findings demonstrated the superior performance of the pre-nCRT radiomic signature, reaching a C-index of 0.724. This elevated performance could likely be attributed to the accuracy and reliability of information extracted from the pre-nCRT MRI images, providing more precise insights into the distinct characteristics of the tumor. Furthermore, in the existing body of knowledge, limited studies have previously delved into the subject of delta radiomic signatures for the prediction of survival in patients with LARC. The resulting data implied that delta radiomic signature had a lower ability to predict DFS, with a C-index of 0.625. This suggests that the delta radiomic signature may not have a strong discriminatory power in predicting DFS in such a population.

In addition to the radiomic analyses, a comprehensive radiomic nomogram was developed, incorporating pre-surgery CEA, post-surgery pathological stage, as well as the pre-nCRT radscore and post-nCRT radscore. This nomogram demonstrated superior performance compared to the clinical models, as evidenced by a higher C-index and positive NRI, as well as lower AIC. These findings are consistent with previous studies in NARC [20, 23, 31]. In addition, in other cancer types such as liver cancer[32], lung cancer[33], as well as cervical cancer[34], the radiomics nomograms based on MRI images also has better predictive performance than their corresponding clinical models. There are two main reasons for this improvement. First, this combination of factors reflects clinical practice and encompasses the entire treatment procedure for rectal cancer. Secondly, clinical and pathological features alone capture limited tumor-specific information,

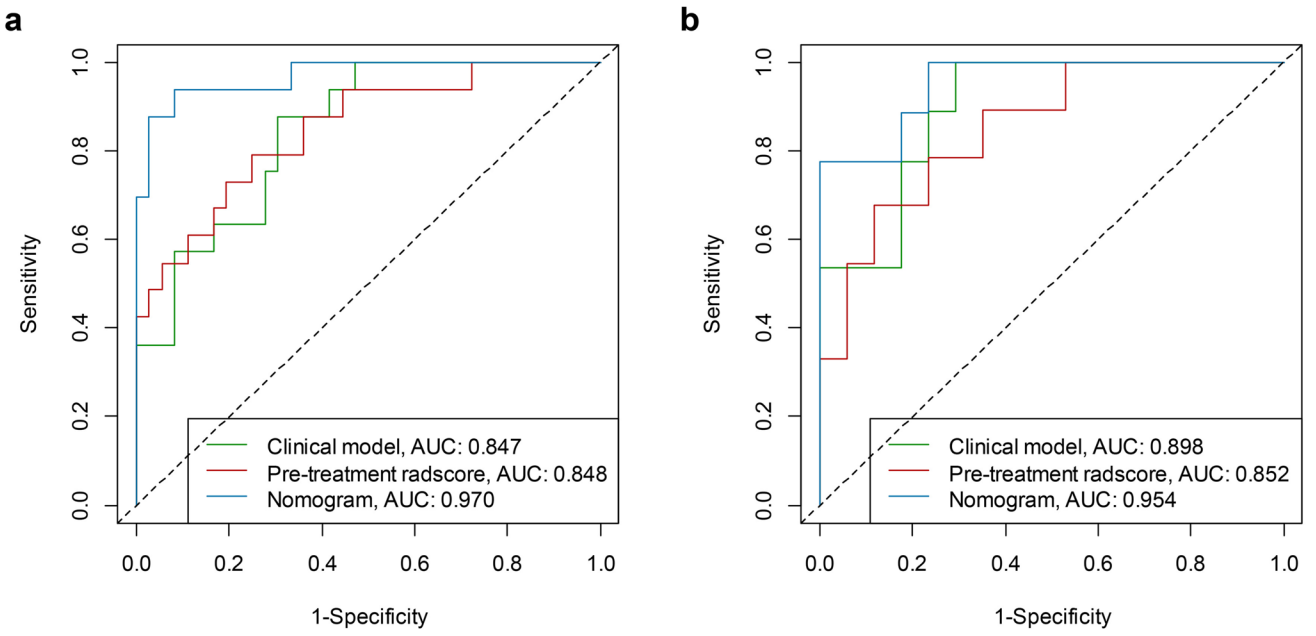

Fig. 4 ROC curves for 5 years in the training set (**a**) and validation cohort (**b**)

whereas MRI-based radiomic offer a comprehensive and quantitative means of characterizing the tumor phenotype. This approach provides a noninvasive avenue for assessing intratumoral heterogeneity, thus enriching our understanding of rectal cancer at a more nuanced level. Furthermore, the strong predictive ability of the radiomic models for DFS confirms their prognostic value, exhibiting effective stratification of patients into high-risk and low-risk groups. Stratified analyses further support these findings, indicating that this approach has the potential to guide more personalized and effective treatments.

Our study has some limitations. First, the single-center design and retrospective nature of the research may introduce selection bias and limit the generalizability of the findings. To address this, multicenter studies are necessary to evaluate the broader applicability and clinical relevance of the model we have developed. Second, although the follow-up period was thorough, it may not have been long enough to provide a more comprehensive analysis of outcomes. As a result, the radiomic model primarily focused on DFS as the primary endpoint. Lastly, while the predictive models were robust, they were limited in scope, incorporating only clinical factors and radiomic features. Other important elements related to tumor biology, such as other imaging modalities, molecular biomarkers, and gene expression profiles, were not included but could offer valuable insights into rectal cancer prognosis and should be considered in future research.

Conclusions

In conclusion, this current study has identified an MRI-based radiomic model as a robust measure to predict prognosis in patients with LARC. This model has significantly enhanced the prognostic capacity of the clinicopathological model, presenting a more comprehensive assessment of outcomes. Furthermore, the established radiomic nomogram efficiently classifies patients into high- and low-risk groups for DFS, thereby offering invaluable guidance for the implementation of precision medicine in LARC patient management. Future endeavors should involve prospective studies, thereby exploring the generalizability and clinical applicability of our constructed models.

Author Contributions JL and KL designed the study. LW, JL, and CF acquired the data. PS-H, QL and XP-Y collected the follow-up data. FB, SY-L and LJ took part in performing image segmentation and data extraction. JM-Z and SL-N developed the model and made statistical analysis. LW contributed significantly to writing the manuscript. All authors read and approved the final manuscript.

Funding This work was supported by the Scientific Research Project of Hunan Provincial Health Commission (project no. 20201028), the National Natural Science Foundation of Hunan (project no. 2021JJ70104), and the China International Medical Foundation (project no. 2-2014-07-1912-22).

Data availability No datasets were generated or analysed during the current study.

Declarations

Competing interests The authors declare no competing interests.

Ethical approval The approval for this retrospective study was granted by the institutional review board of our hospital.

References

1. Sung, H., J. Ferlay, R.L. Siegel, M. Laversanne, I. Soerjomataram, A. Jemal, and F. Bray (2021) Global Cancer Statistics 2020: GLOBOCAN estimates of incidence and mortality worldwide for 36 Cancers in 185 Countries. CA Cancer J Clin 71(3). https://https://doi.org/10.3322/caac.21660
2. Siegel, R.L., K.D. Miller, S.A. Fedewa, D.J. Ahnen, R.G.S. Meester, A. Barzi, and A. Jemal (2017) Colorectal cancer statistics, 2017. CA Cancer J Clin 67(3). https://https://doi.org/10.3322/caac.21395
3. Valentini, V., C. Aristei, B. Glimelius, B.D. Minsky, R. Beets-Tan, J.M. Borras, K. Haustermans, P. Maingon, J. Overgaard, L. Pahlman, P. Quirke, H.J. Schmoll, D. Sebag-Montefiore, I. Taylor, E. Van Cutsem, C. Van de Velde, N. Cellini, P. Latini, and C. Scientific (2009) Multidisciplinary rectal cancer management: 2nd European rectal cancer consensus conference (EURECA-CC2). Radiother Oncol 92(2). https://https://doi.org/10.1016/j.radonc.2009.06.027
4. Rodel, C., T. Liersch, H. Becker, R. Fietkau, W. Hohenberger, T. Hothorn, U. Graeven, D. Arnold, M. Lang-Welzenbach, H.R. Raab, H. Sulberg, C. Wittekind, S. Potapov, L. Staib, C. Hess, K. Weigang-Kohler, G.G. Grabenbauer, H. Hoffmanns, F. Lindemann, A. Schlenska-Lange, G. Folprecht, R. Sauer, and G. German Rectal Cancer Study (2012) Preoperative chemoradiotherapy and postoperative chemotherapy with fluorouracil and oxaliplatin versus fluorouracil alone in locally advanced rectal cancer: initial results of the German CAO/ARO/AIO-04 randomised phase 3 trial. Lancet Oncol 13(7). https://https://doi.org/10.1016/S1470-2045(12)70187-0
5. Van Gijn, W., C.A. Marijnen, I.D. Nagtegaal, E.M. Kranenbarg, H. Putter, T. Wiggers, H.J. Rutten, L. Pahlman, B. Glimelius, C.J. van de Velde, and G. Dutch Colorectal Cancer (2011) Preoperative radiotherapy combined with total mesorectal excision for resectable rectal cancer: 12-year follow-up of the multicentre, randomised controlled TME trial. Lancet Oncol 12(6). https://https://doi.org/10.1016/S1470-2045(11)70097-3
6. Valentini, V., R.G. van Stiphout, G. Lammering, M.A. Gambacorta, M.C. Barba, M. Bebenek, F. Bonnetain, J.F. Bosset, K. Bujko, L. Cionini, J.P. Gerard, C. Rodel, A. Sainato, R. Sauer, B.D. Minsky, L. Collette, and P. Lambin (2011) Nomograms for predicting local recurrence, distant metastases, and overall survival for patients with locally advanced rectal cancer on the basis of European randomized clinical trials. J Clin Oncol 29(23). https://https://doi.org/10.1200/JCO.2010.33.1595
7. Hong, Y.S., B.H. Nam, K.P. Kim, J.E. Kim, S.J. Park, Y.S. Park, J.O. Park, S.Y. Kim, T.Y. Kim, J.H. Kim, J.B. Ahn, S.B. Lim, C.S. Yu, J.C. Kim, S.H. Yun, J.H. Kim, J.H. Park, H.C. Park, K.H. Jung, and T.W. Kim (2014) Oxaliplatin, fluorouracil, and leucovorin versus fluorouracil and leucovorin as adjuvant chemotherapy for locally advanced rectal cancer after preoperative chemoradiotherapy (ADORE): an open-label, multicentre, phase 2, randomised controlled trial. Lancet Oncol 15(11). https://https://doi.org/10.1016/S1470-2045(14)70377-8
8. Polanco, P.M., A.A. Mokdad, H. Zhu, M.A. Choti, and S. Huerta (2018) Association of adjuvant chemotherapy with overall survival in patients with rectal cancer and pathologic complete response following neoadjuvant chemotherapy and resection. JAMA Oncol 4(7). https://https://doi.org/10.1001/jamaoncol.2018.0231
9. Maas., M., P.J. Nelemans., V. Valentini., C.H. Crane., C. Capirci., and C. Rodel. (2015) Adjuvant chemotherapy in rectal cancer: defining subgroups who may benefit after neoadjuvant chemoradiation and resection: a pooled analysis of 3,313 patients - PubMed. International journal of cancer 137(1). https://https://doi.org/10.1002/ijc.29355
10. Sun, Y., H. Lin, X. Lu, Y. Huang, Z. Xu, S. Huang, X. Wang, and P. Chi (2017) A nomogram to predict distant metastasis after neoadjuvant chemoradiotherapy and radical surgery in patients with locally advanced rectal cancer. J Surg Oncol 115(4). https://https://doi.org/10.1002/jso.24522
11. Merkel, S., K. Weber, V. Schellerer, J. Gohl, R. Fietkau, A. Agaimy, W. Hohenberger, and P. Hermanek (2014) Prognostic subdivision of ypT3 rectal tumours according to extension beyond the muscularis propria. Br J Surg 101(5). https://https://doi.org/10.1002/bjs.9419
12. Kim, W.R., Y.D. Han, and B.S. Min (2018) C-reactive protein level predicts survival outcomes in rectal cancer patients undergoing total mesorectal excision after preoperative chemoradiation therapy. Ann Surg Oncol 25(13). https://https://doi.org/10.1245/s10434-018-6828-4
13. Fokas, E., T. Liersch, R. Fietkau, W. Hohenberger, T. Beissbarth, C. Hess, H. Becker, M. Ghadimi, K. Mrak, S. Merkel, H.R. Raab, R. Sauer, C. Wittekind, and C. Rodel (2014) Tumor regression grading after preoperative chemoradiotherapy for locally advanced rectal carcinoma revisited: updated results of the CAO/ARO/AIO-94 trial. J Clin Oncol 32(15). https://https://doi.org/10.1200/JCO.2013.54.3769
14. Conroy, T., J.F. Bosset, P.L. Etienne, E. Rio, E. Francois, N. Mesgouez-Nebout, V. Vendrely, X. Artignan, O. Bouche, D. Gargot, V. Boige, N. Bonichon-Lamichhane, C. Louvet, C. Morand, C. de la Fouchardiere, N. Lamfichekh, B. Juzyna, C. Jouffroy-Zeller, E. Rullier, F. Marchal, S. Gourgou, F. Castan, C. Borg, G. Unicancer Gastrointestinal, and G. Partenariat de Recherche en Oncologie Digestive (2021) Neoadjuvant chemotherapy with FOLFIRINOX and preoperative chemoradiotherapy for patients with locally advanced rectal cancer (UNICANCER-PRODIGE 23): a multicentre, randomised, open-label, phase 3 trial. Lancet Oncol 22(5). https://https://doi.org/10.1016/S1470-2045(21)00079-6
15. Bahadoer, R.R., E.A. Dijkstra, B. van Etten, C.A.M. Marijnen, H. Putter, E.M. Kranenbarg, A.G.H. Roodvoets, I.D. Nagtegaal, R.G.H. Beets-Tan, L.K. Blomqvist, T. Fokstuen, A.J. Ten Tije, J. Capdevila, M.P. Hendriks, I. Edhemovic, A. Cervantes, P.J. Nilsson, B. Glimelius, C.J.H. van de Velde, G.A.P. Hospers, and R.c. investigators (2021) Short-course radiotherapy followed by

chemotherapy before total mesorectal excision (TME) versus preoperative chemoradiotherapy, TME, and optional adjuvant chemotherapy in locally advanced rectal cancer (RAPIDO): a randomised, open-label, phase 3 trial. Lancet Oncol 22(1). https://https://doi.org/10.1016/S1470-2045(20)30555-6
16. Jin, J., Y. Tang, C. Hu, L.M. Jiang, J. Jiang, N. Li, W.Y. Liu, S.L. Chen, S. Li, N.N. Lu, Y. Cai, Y.H. Li, Y. Zhu, G.H. Cheng, H.Y. Zhang, X. Wang, S.Y. Zhu, J. Wang, G.F. Li, J.L. Yang, K. Zhang, Y. Chi, L. Yang, H.T. Zhou, A.P. Zhou, S.M. Zou, H. Fang, S.L. Wang, H.Z. Zhang, X.S. Wang, L.C. Wei, W.L. Wang, S.X. Liu, Y.H. Gao, and Y.X. Li (2022) Multicenter, randomized, phase III trial of short-term radiotherapy plus chemotherapy versus long-term chemoradiotherapy in locally advanced rectal cancer (STELLAR). J Clin Oncol 40(15). https://https://doi.org/10.1200/JCO.21.01667
17. Hatt, M., F. Tixier, D. Visvikis, and C. Cheze Le Rest (2017) Radiomics in PET/CT: more than meets the eye? J Nucl Med 58(3). https://https://doi.org/10.2967/jnumed.116.184655
18. Kuo, M.D. and N. Jamshidi (2014) Behind the numbers: decoding molecular phenotypes with radiogenomics--guiding principles and technical considerations. Radiology 270(2). https://https://doi.org/10.1148/radiol.13132195
19. Gevaert, O., J. Xu, C.D. Hoang, A.N. Leung, Y. Xu, A. Quon, D.L. Rubin, S. Napel, and S.K. Plevritis (2012) Non-small cell lung cancer: identifying prognostic imaging biomarkers by leveraging public gene expression microarray data--methods and preliminary results. Radiology 264(2). https://https://doi.org/10.1148/radiol.12111607
20. Cui, Y., G. Wang, J. Ren, L. Hou, D. Li, Q. Wen, Y. Xi, and X. Yang (2022) Radiomics features at multiparametric MRI predict disease-free survival in patients with locally advanced rectal cancer. Acad Radiol 29(8). https://https://doi.org/10.1016/j.acra.2021.11.024
21. Wang, F., B.F. Tan, S.S. Poh, T.R. Siow, F. Lim, C.S.P. Yip, M.L.C. Wang, W. Nei, and H.Q. Tan (2022) Predicting outcomes for locally advanced rectal cancer treated with neoadjuvant chemoradiation with CT-based radiomics. Sci Rep 12(1). https://https://doi.org/10.1038/s41598-022-10175-2
22. Tibermacine, H., P. Rouanet, M. Sbarra, R. Forghani, C. Reinhold, S. Nougaret, and G.S. Group (2021) Radiomics modelling in rectal cancer to predict disease-free survival: evaluation of different approaches. Br J Surg 108(10). https://https://doi.org/10.1093/bjs/znab191
23. Cui, Y., W. Yang, J. Ren, D. Li, X. Du, J. Zhang, and X. Yang (2021) Prognostic value of multiparametric MRI-based radiomics model: potential role for chemotherapeutic benefits in locally advanced rectal cancer. Radiother Oncol 154. https://https://doi.org/10.1016/j.radonc.2020.09.039
24. Li, M., Y.Z. Zhu, Y.C. Zhang, Y.F. Yue, H.P. Yu, and B. Song (2020) Radiomics of rectal cancer for predicting distant metastasis and overall survival. World J Gastroenterol 26(33). https://https://doi.org/10.3748/wjg.v26.i33.5008
25. Wen, L., J. Liu, P. Hu, F. Bi, S. Liu, L. Jian, S. Zhu, S. Nie, F. Cao, Q. Lu, X. Yu, and K. Liu (2023) MRI-based radiomic models outperform radiologists in predicting pathological complete response to neoadjuvant chemoradiotherapy in locally advanced rectal cancer. Acad Radiol 30 Suppl 1. https://https://doi.org/10.1016/j.acra.2022.12.037
26. Jalil, O., A. Afaq, B. Ganeshan, U.B. Patel, D. Boone, R. Endozo, A. Groves, B. Sizer, and T. Arulampalam (2017) Magnetic resonance based texture parameters as potential imaging biomarkers for predicting long-term survival in locally advanced rectal cancer treated by chemoradiotherapy. Colorectal Dis 19(4). https://https://doi.org/10.1111/codi.13496
27. Lovinfosse, P., M. Polus, D. Van Daele, P. Martinive, F. Daenen, M. Hatt, D. Visvikis, B. Koopmansch, F. Lambert, C. Coimbra, L. Seidel, A. Albert, P. Delvenne, and R. Hustinx (2018) FDG PET/CT radiomics for predicting the outcome of locally advanced rectal cancer. Eur J Nucl Med Mol Imaging 45(3). https://https://doi.org/10.1007/s00259-017-3855-5
28. Stollfuss, J.C., K. Becker, A. Sendler, S. Seidl, M. Settles, F. Auer, A. Beer, E.J. Rummeny, and K. Woertler (2006) Rectal carcinoma: high-spatial-resolution MR imaging and T2 quantification in rectal cancer specimens. Radiology 241(1). https://https://doi.org/10.1148/radiol.2411050942
29. Treiber, J.M., N.S. White, T.C. Steed, H. Bartsch, D. Holland, N. Farid, C.R. McDonald, B.S. Carter, A.M. Dale, and C.C. Chen (2016) Characterization and correction of geometric distortions in 814 diffusion weighted images. PLoS One 11(3). https://https://doi.org/10.1371/journal.pone.0152472
30. Tao, R., P.T. Fletcher, S. Gerber, and R.T. Whitaker (2009) A variational image-based approach to the correction of susceptibility artifacts in the alignment of diffusion weighted and structural MRI. Inf Process Med Imaging 21. https://https://doi.org/10.1007/978-3-642-02498-6_55
31. Liu, Z., X. Meng, H. Zhang, Z. Li, J. Liu, K. Sun, Y. Meng, W. Dai, P. Xie, Y. Ding, M. Wang, G. Cai, and J. Tian (2020) Predicting distant metastasis and chemotherapy benefit in locally advanced rectal cancer. Nat Commun 11(1). https://https://doi.org/10.1038/s41467-020-18162-9
32. Zhao, Y., F. Huang, S. Liu, L. Jian, X. Xia, H. Lin, and J. Liu (2023) Prediction of therapeutic response of unresectable hepatocellular carcinoma to hepatic arterial infusion chemotherapy based on pretherapeutic MRI radiomics and Albumin-Bilirubin score. J Cancer Res Clin Oncol 149(8). https://https://doi.org/10.1007/s00432-022-04467-3
33. Xie, K., C. Cui, X. Li, Y. Yuan, Z. Wang, and L. Zeng (2024) MRI-based clinical-imaging-radiomics nomogram model for discriminating between benign and malignant solid pulmonary nodules or masses. Acad Radiol 31(10). https://https://doi.org/10.1016/j.acra.2024.03.042
34. Lin, Y., Y. Gao, and T. Weng (2024) Construction and validation of a MRI-based radiomic nomogram to predict overall survival in patients with local advanced cervical cancer: a multicenter study. Acad Radiol 31(11). https://https://doi.org/10.1016/j.acra.2024.05.003

Authors and Affiliations

Jun Liu[1] · Ke Liu[2] · Fang Cao[3] · Pingsheng Hu[1] · Feng Bi[1] · Siye Liu[1] · Lian Jian[1] · Jumei Zhou[2] · Shaolin Nie[4] · Qiang Lu[1] · Xiaoping Yu[1] · Lu Wen[1]

✉ Lu Wen
wenlu@hnca.org.cn

Jun Liu
liujun2386@hnca.org.cn

Ke Liu
liuke@hnca.org.cn

Fang Cao
caofang@hnca.org.cn

Pingsheng Hu
hupingsheng@hnca.org.cn

Feng Bi
bifeng@hnca.org.cn

Siye Liu
liusiye@hnca.org.cn

Lian Jian
jianlian@hnca.org.cn

Jumei Zhou
zhoujumei@hnca.org.cn

Shaolin Nie
nieshaolin@hnca.org.cn

Qiang Lu
luqiang@hnca.org.cn

Xiaoping Yu
yuxiaoping@hnca.org.cn

[1] Department of Diagnostic Radiology, Hunan Cancer Hospital and the Affiliated Cancer Hospital of Xiangya School of Medicine, Central South University, Changsha, Hunan, People's Republic of China

[2] Department of Radiotherapy, Hunan Cancer Hospital and the Affiliated Cancer Hospital of Xiangya School of Medicine, Central South University, Changsha, Hunan, People's Republic of China

[3] Department of Pathology, Hunan Cancer Hospital and the Affiliated Cancer Hospital of Xiangya School of Medicine, Central South University, Changsha, Hunan, People's Republic of China

[4] Department of Colorectal Surgery, Hunan Cancer Hospital and the Affiliated Cancer Hospital of Xiangya School of Medicine, Central South University, Changsha, Hunan, People's Republic of China